# Achievable rate degradation of ultra-wideband coherent fiber communication systems due to stimulated Raman scattering

**DANIEL SEMRAU,[1,*] ROBERT KILLEY,[1] AND POLINA BAYVEL[1]**

[1] *Optical Networks Group (ONG), Department of Electronic & Electrical Engineering, UCL (University College London), Torrington Place, London WC1E 7JE, UK*
[*] *daniel.semrau.15@ucl.ac.uk*

**Abstract:** As the bandwidths of optical communication systems are increased to maximize channel capacity, the impact of stimulated Raman scattering (SRS) on the achievable information rates (AIR) in ultra-wideband coherent WDM systems becomes significant, and is investigated in this work, for the first time. By modifying the GN-model to account for SRS, it is possible to derive a closed-form expression that predicts the optical signal-to-noise ratio of all channels at the receiver for bandwidths of up to 15 THz, which is in excellent agreement with numerical calculations. It is shown that, with fixed modulation and coding rate, SRS leads to a drop of approximately 40% in achievable information rates for bandwidths higher than 15 THz. However, if adaptive modulation and coding rates are applied across the entire spectrum, this AIR reduction can be limited to only 10%.



**OCIS codes:** (060.0060) Fiber optics and optical communications; (190.4370) Nonlinear optics, fibers; (190.3270) Kerr effect; (190.4223) Nonlinear wave mixing; (190.5650) Raman effect; (190.5890) Scattering, stimulated.

## References and links

1. E. M. Dianov, "Amplification in extended transmission bands using Bismuth-doped optical fibers," J. Lightwave Technol. **31**(4), 681–688 (2013).
2. J. Bromage, "Raman amplification for fiber communications systems," J. Lightwave Technol. **22**(1), 79–93 (2004).
3. R. H. Stolen and E. P. Ippen, "Raman gain in glass optical waveguides," Appl. Phys. Lett. **22**(6), 276–278 (1973).
4. A. R. Chraplyvy, "Limitations on lightwave communications imposed by optical-fiber nonlinearities," J. Lightwave Technol. **8**(2), 1548–1557 (1990).
5. A. R. Chraplyvy, "Optical power limits in multi-channel wavelength-division-multiplexed systems due to stimulated Raman scattering," Electron. Lett. **20**(2), 58–59 (1984).
6. H. D. Kim and C. H. Lee, "Capacities of WDM transmission systems and networks limited by stimulated Raman scattering," IEEE Photonics Technol. Lett. **13**(4), 379–381 (2001).
7. A. R. Sarkar, M. N. Islam and M. G. Mostafa, "Performance of an optical wideband WDM system considering stimulated Raman scattering, fiber attenuation and chromatic dispersion," Opt. Quant. Electron. **39**(8), 659–675 (2007).
8. A. G. Grandpierre, D. N. Christodoulides, and J. Toulouse, "Theory of stimulated Raman scattering cancellation in wavelength-division-multiplexed systems via spectral inversion," IEEE Photonics Technol. Lett. **11**(10), 1271–1273 (1999).
9. P. Dong, X. Xiao, Y. Tian, S. Gao, and C. Yang, "Compensating power depletion due to stimulated Raman scattering in high-power delivery fiber via spectral inversion," J. Opt. Soc. Am. B **25**(1), 48–53 (2008).
10. Y. Wang, C. Q. Xu, and H. Po, "Analysis of Raman and thermal effects in kilowatt fiber lasers," Opt. Commun. **242**(4-6), 487–502 (2004).
11. J. M. Fini, M. D. Mermelstein, M. F. Yan, R. T. Bise, A. D. Yablon, P. W. Wisk, and M. J. Andrejo, "Distributed suppression of stimulated Raman scattering in an Yb-doped filter-fiber amplifier," Opt. Lett. **31**(1), 2550–2552 (2006).
12. J. Kim, D. Dubriez, C. Codemard, J. Nilsson, and J. K. Sahu, "Suppression of stimulated Raman scattering in a high power Yb-doped fiber amplifier using a W-type core with fundamental mode cut-off," Opt. Express **14**(12), 5103–5113 (2006).
13. S. Norimatsu and T. Yamamoto, "Waveform distortion due to stimulated Raman scattering in wide-band WDM transmission systems," J. Lightwave Technol. **19**(2), 159–171 (2001).
14. F. Forghieri, R. W. Tkach, and A. R. Chraplyvy, "Effect of modulation statistics on Raman crosstalk in WDM systems," IEEE Photonics Technol. Lett. **7**(1), 101–103 (1995).

15. J. Wang, X. Sun, and M. Zhang, "Effect of group velocity dispersion on stimulated Raman crosstalk in multichannel transmission systems," IEEE Photonics Technol. Lett. **10**(4), 540–542 (1998).
16. S. Tariq and J. C. Palais, "A computer model of non-dispersion-limited stimulated Raman scattering in optical fiber multiple-channel communications," J. Lightwave Technol. **11**(12), 1914–1924 (1993).
17. L. Qiang and G. P. Agrawal, "Vector theory of stimulated Raman scattering and its application to fiber-based Raman amplifiers," J. Opt. Soc. Am. B **20**(8), 1616–1631 (2003).
18. P. Poggiolini, G. Bosco, A. Carena, V. Curri, Y. Jiang, and F. Forghieri, "The GN-Model of fiber non-linear propagation and its applications," J. Lightwave Technol. **32**(4), 694–721 (2014).
19. J. Cai, H.G. Batshon, H. Zhang, M. Mazurczyk, O. Sinkin, D. Foursa, and A. Pilipetskii, "Transmission performance of coded modulation formats in a wide range of spectral efficiencies," in *Proceedings of OFC 2014* (2014), paper M2C.3.
20. R. Dar, M. Feder, A. Mercozzi, and M. Shtaif, "Accumulation of nonlinear interference noise in fiber-optic systems," Opt. Express **22**(12), 14199–14211 (2014).
21. R. Dar, O. Geller, M. Feder, A. Mercozzi, and M. Shtaif, "Mitigation of inter-channel nonlinear interference in WDM systems," in *Proceedings of ECOC 2014* (2014).
22. A. D. Ellis et al. "4 Tb/s Transmission Reach Enhancement Using 10 × 400 Gb/s Super-Channels and Polarization Insensitive Dual Band Optical Phase Conjugation," J. Lightwave Technol. **34**(8), 1717–1723 (2016).
23. C. E. Shannon, "A mathematical theory of communication," Bell Sys. Tech. J. **27**, 379–423 (1948).
24. A. Ghazisaeidi, I. F. Ruiz, L. Schmalen, P. Tran, C. Simonneau, Elie Awwad, B. Uscumlic, P. Brindel, and G. Charlet, "Submarine transmission systems using digital nonlinear compensation and adaptive rate forward error correction," J. Lightwave Technol. **34**(8), 1886–1895 (2016).
25. J. X. Cai, Y. Sun. H. Zhang, H. Batshon, M. Mazurczyk, O. Sinkin, D. Foursa, and A. Pilipetskii, "High-speed and transoceanic distance transmission with hybrid Raman-EDFA and coded modulation," in *Proceedings of ECOC 2015* (2015).
26. R. Maher, T. Xu, L. Galdino, M. Sato, A. Alvarado, K. Shi, Seb. J. Savory, B. C. Thomsen, R. I. Killey, and P. Bayvel, "Spectrally shaped DP-16QAM super-channel transmission with multi-channel digital back-propagation," Sci. Rep. **5**, 8214 (2015).
27. L. Galdino, M. Tan, A. Alvarado, D. Lavery, P. Rosa, R. Maher, J. D. Castañón, P. Harper, S. Makovejs, B. C. Thomsen, and P. Bayvel, "Amplification schemes and multi-channel DBP for unrepeatered transmission," J. Lightwave Technol. **34**(9), 2221–2227 (2016).
28. M. Zirngibl, "Analytical model of Raman gain effects in massive wavelength division multiplexed transmission systems," Electron. Lett. **34**(8), 789–790 (1998).

## 1. Introduction

Increasing the bandwidth of optical communication systems is vital to maximize optical fiber channel capacity, as data demand continues on its rapid growth trend. In recent years much attention has been focused on the study and mitigation of Kerr nonlinearities (including the effects of SPM, XPM and FWM) which limit the achievable data rates within the relatively small bandwidths of 5-10 THz and below, as defined by C- and L- gain bandwidths over which Erbium fiber amplifiers operate. Increasing the transmission bandwidths further to make greater use of the available optical fiber bandwidth is now viewed as a highly promising approach to increase channel throughput. This depends on the availability of ultra-wideband optical amplifiers with potential technologies including, for example, Bismuth-doped fiber [1] or Raman amplifiers [2], both of which may allow significant increases in bandwidths. However, any significant bandwidth increases require the analysis of limits on the achievable information rates imposed by fiber nonlinearities.

To date, very little analysis of the impact of bandwidth increases on the scaling of nonlinear effects has been carried out in coherent WDM optical transmission systems. Since the impact of the Kerr effect decreases with frequency spacing due to the chromatic dispersion induced walk-off between the interacting spectral components, the additional signal distortions due to the Kerr effect will become less severe with increases in signal bandwidth. However, stimulated Raman scattering (SRS) leads to a power transfer from higher to lower frequencies, increasing in strength with wider frequency separation (up to approximately 15 THz for a standard single mode fiber). Figure 1 shows the Raman gain coefficient for frequency separations up to 20 THz, as measured by Stolen and Ippen in 1973 [3].

In the early studies of non-coherent optical fiber transmission it was suggested that the effect of

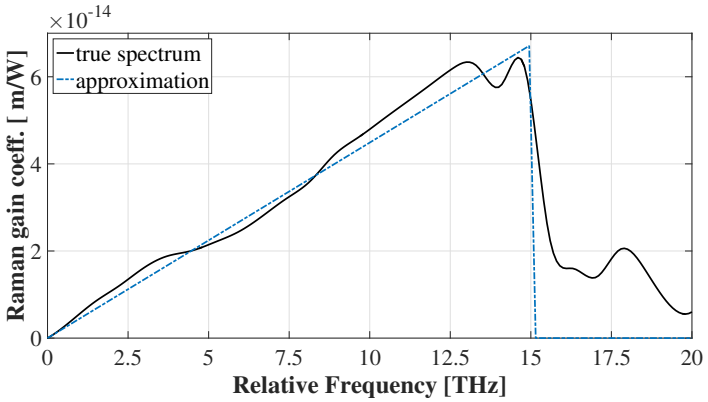


Fig. 1. Raman spectrum at 1550 nm for a standard single mode fiber (see [3]).

SRS cannot be neglected when operating over very large bandwidths and mitigation techniques would be needed [4–7]. To date, the impact of SRS has not been relevant for practical systems operating over bandwidths less than 5 THz. However, as bandwidths increase in the quest to increase channel throughput, the impact of stimulated Raman scattering must be revisited in the context of exploring its impact on achievable communications rates in coherent WDM communication systems. In almost all cases considered to date (which mainly concern the very early studies mentioned above), the contribution of the Kerr nonlinearity was neglected and a linear approximation of the Raman gain was assumed limiting the results to bandwidths of 15 THz and below. To our knowledge the impact of SRS on the achievable information rates of coherent WDM transmission systems that exploit higher order modulation formats is yet to be reported.

Besides the modeling of the SRS effect, methods to mitigate this effect have been investigated. Spectral inversion in the middle of each span to revert the power flow in the latter half of the span is one of the suggested compensation methods [8, 9]. Other proposals adjust the fiber parameters such as core area and core design, or reduce the amplifier span length, such that the effects of stimulated Raman scattering are decreased [10–12]. However, in practice, these approaches would require major hardware changes.

In this paper, for the first time, the achievable information rate analysis is carried out for coherent, ultra-wideband Nyquist WDM communication systems with both SRS and Kerr effects exploiting the Gaussian noise (GN) model. A new closed-form expression which describes the optical signal-to-noise ratio (OSNR) distribution at the receiver in a system with optimized wavelength-dependent gain is derived. This closed-form expression is compared to numerical calculations, with excellent agreement between the two. Application of adaptive modulation formats and coding rates, continuously varying across the wavelength spectrum, is proposed as a flexible SRS mitigation technique and is shown to lead to substantial increases in achievable information rates, without requiring any significant changes to the installed fiber infrastructure.

## 2. The system model

Stimulated Raman scattering amplifies low frequency channels in phase and depletes the corresponding high frequency channels accordingly. This process can be separated into two contributions, namely an average power gain (or loss) and a modulation dependent cross-talk component [13]. In the context of coherent, highly dispersive, densely spaced WDM systems a single pulse in a low frequency channel interacts with many high frequency channels during propagation. This results in averaging and a more deterministic behavior of the modulation

transfer. This averaging has been shown in the context of on-off keying systems [14, 15]. In this work, only the average SRS gain and loss contribution is considered and the modulation dependent cross-talk is neglected and left for future studies. To numerically calculate the power exchange due to SRS, the model given by Tariq and Palais was used [16]. The power evolution of an individual channel $i$ is then given by a set of $M$ coupled differential equations, where $M$ is the total number of channels

$$\frac{\partial P_i}{\partial z} = \underbrace{-\sum_{j=i+1}^{M} \frac{\omega_j}{2\omega_i} g_R(\Omega) P_j P_i}_{\text{SRS loss}} + \underbrace{\sum_{j=1}^{i-1} \frac{1}{2} g_R(\Omega) P_j P_i}_{\text{SRS gain}} - \alpha P_i, \tag{1}$$

with the optical power $P_i$, of channel $i$, the normalized Raman gain coefficient $g_R(\Omega)$, the attenuation coefficient $\alpha$ and the frequency separation $\Omega = |f_j - f_i|$ between channel $j$ and $i$. The factor $\frac{\omega_j}{\omega_i}$ conserves the photon number and the factor $\frac{1}{2}$ accounts for polarization averaging as the Raman gain coefficient is strongly polarization dependent [17]. The channels are indexed such that the highest frequency channel has index $i = 1$.

It is assumed that after every span the power tilt across the spectrum is perfectly corrected by the use of a discrete amplifier with an appropriate gain profile (e.g., through the use of a gain flattening filter). This will effectively amplify every channel corresponding to its respective loss. In practice, the amplification may be carried out in bands, with multiple amplifiers in parallel but, in this analysis, continuous gain across the spectrum was assumed. The logarithmic gain of the amplifier is considered to be the sum of the logarithmic gain $g_{\text{u}}$, required to compensate the linear loss of the fiber span (assumed to be uniform across the signal spectrum) and the logarithmic gain $g_{\text{nu},i}$, that offsets the non-uniform and channel dependent gain or loss due to SRS. This discrete amplification gives rise to channel dependent amplified spontaneous emission (ASE) noise of power $P_{\text{ASE},i}$. This noise contribution is added at each span and given by

$$P_{\text{ASE},i} = FhfB_{\text{ch}}\exp(g_{\text{u}} - g_{\text{nu},i}), \tag{2}$$

with noise figure $F$, Planck's constant $h$, frequency $f$, channel bandwidth $B_{\text{ch}}$, the uniform logarithmic gain contribution $g_{\text{u}} = aL$ with span length $L$ and the non-uniform logarithmic gain contribution $g_{\text{nu},i}$ due to SRS. The quantity $g_{\text{nu},i}$ can be computed as

$$g_{\text{nu},i} = \ln\left[\frac{P_i(L)}{P_i(0)\exp(-\alpha L)}\right]. \tag{3}$$

The power evolution of every channel was calculated for a span length, $L$ of 100 km by numerically solving Eq. (1) with the Runge-Kutta method. For all calculations in this paper ideal dual-polarization coherent transceivers were assumed. A fully loaded (ideal Nyquist-spaced) WDM signal with a total example bandwidth, $B_{\text{tot}}$ of 10 THz, channel bandwidth, $B_{\text{ch}}$ of 10 GHz and an effective fiber core area, $A_{\text{eff}}$ of 80 $\mu\text{m}^2$ was assumed. The resulting power evolution over two spans is shown in Fig. 2. For these parameters the optimum launch power can be obtained from the GN-model. The GN-model (which does not include SRS) treats the Kerr effect as a perturbation and defines nonlinear distortion through a nonlinear interference (NLI) coefficient $\eta_i$ for channel $i$ [18]. Recently, the GN model has been experimentally validated for a total optical bandwidth of 41.5 nm / 5 THz [19]. The nonlinear interference is assumed to remain circular-additive Gaussian for wider bandwidths as the impact of phase noise and polarization rotation noise is typically negligible in long-haul lumped-amplified links that exhibit long span lengths [20,21]. In this work we assumed a uniform optimal power across the spectrum and denote this power by $P_0$. It is further assumed that signal-noise interactions are negligible. Similar to [22], the signal-noise interactions could be included with an additional noise term

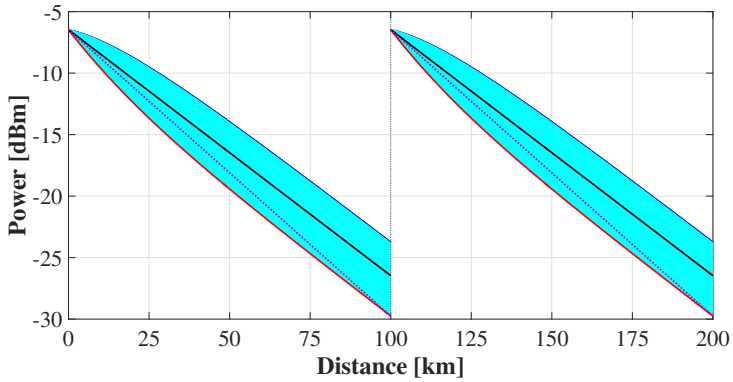


Fig. 2. Power evolution of each channel in a 10 THz WDM signal. Legend: —— Highest frequency channel. —— Central frequency channel. —— Lowest frequency channel. ····· Linear approximation of highest frequency channel.

of $3\eta_i \sum_{k=1}^{N_s} k P_{\mathrm{ASE},i} P^2$, with the number of spans $N_s$ and launch power $P$. However, for moderate launch powers, this contribution can be neglected compared to signal-signal interactions. Although, the signal-signal interactions (proportional to $P^3$) decrease faster for lower launch powers than signal-noise interactions for (proportional to $P^2$), they can still be neglected due to the dominance of the linear ASE noise contribution. When signal-noise interactions are neglected, the optimum launch power per channel is given by [18]

$$P_0 = \left[ \frac{P_{\mathrm{ASE,lin}}}{2\eta_0} \right]^{\frac{1}{3}}, \tag{4}$$

with the nonlinear interference noise coefficient for the central channel $\eta_0$ and the linear amplifier noise component $P_{\mathrm{ASE,lin}}$ that is obtained when $g_{\mathrm{nu},i}$ is set to zero in Eq. (2). When SRS becomes more dominant the optimum launch power is lower than the one predicted by Eq. (4).

To fully account for the combined effects of the Kerr effect and SRS, the GN model needs to be re-derived based on a second-order pertubation method with the SRS term included in the Manakov equation. Due to the second-order requirement, the resulting expressions are computationally too complex to be numerically integrated over the bandwidths considered in this paper. We propose an alternative approach to include SRS induced modifications on the Kerr effect based on an effective attenuation coefficient $\alpha_{\mathrm{eff},i}$ in order to calculate the NLI coefficient $\eta_i$. The effective attenuation coefficient is chosen such that it matches the actual effective length of channel $i$ under the influence of SRS and is computed by solving

$$L_{\mathrm{eff},i} = \int_0^L \frac{P_i(z)}{P_0} dz = \frac{1 - \exp(-\alpha_{\mathrm{eff},i} L)}{\alpha_{\mathrm{eff},i}}, \tag{5}$$

with $P_i(z)$ from Eq. (1). This approach is reasonable as the main contribution of the Kerr effect arises from closely neighboring channels that exhibit a similar effective length. The Kerr-nonlinearity distortion (or nonlinear interference) can be calculated as

$$P_{\mathrm{NLIN},i} = \eta_i P_0^3. \tag{6}$$

Figure 3 shows the noise components of the amplifier and the nonlinear interference after one span with and without SRS. The following parameters were used for the calculations: noise figure $F = 5$ dB, attenuation coefficient $a = 0.2$ dB km$^{-1}$, group velocity dispersion

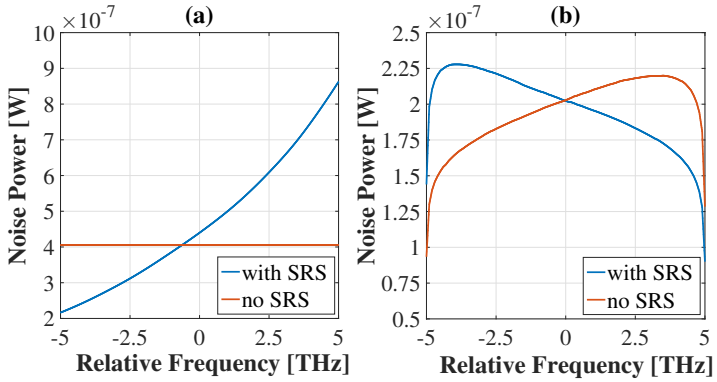


Fig. 3. (a) Noise power of the amplifier. (b) Noise power due to the Kerr effect.

$\beta_2 = -21.3$ ps$^2$ km$^{-1}$, group velocity dispersion slope $\beta_3 = 0.145$ ps$^3$ km$^{-1}$, span length $L = 100$ km and nonlinear coefficient $\gamma = 1.2$ W$^{-1}$ km$^{-1}$. Neglecting signal-noise interactions and assuming that the noise adds incoherently at every span, the optical signal-to-noise-ratio after $N_s$ spans can be obtained using

$$OSNR_i = \frac{P_0}{P_{\mathrm{NLIN},i} + P_{\mathrm{ASE},i}} \frac{1}{N_s}, \tag{7}$$

where the OSNR is taken with a resolution bandwidth equal to the channel bandwidth, $B_{ch}$ of 10 GHz. The effect of spontaneous Raman scattering was neglected as this effect was found to be extremely small compared to all other noise contributions. The OSNR and the maximum achievable spectral efficiency (using adaptive modulation and coding rate, and assuming the throughput limit given by the Shannon-Hartley capacity formula [23]) for a 10 THz WDM signal after 30 spans are shown in Figs. 4 and 5, respectively. When SRS is absent the OSNR is

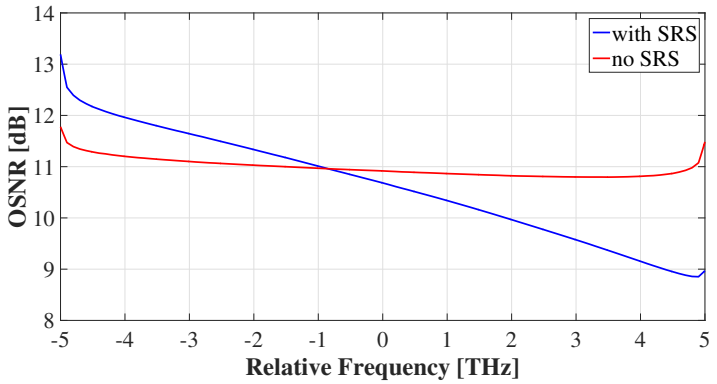


Fig. 4. OSNR of each channel in a 10 THz WDM signal with a resolution bandwidth of 10 GHz at 3000 km.

approximately flat across the entire spectrum and maximum spectral efficiency can be achieved by applying one modulation format and one coding rate for all channels. However, this is not the case in presence of SRS because of a channel dependent OSNR. In order to still achieve maximum spectral efficiency across the spectrum and hence maximize throughput, we propose

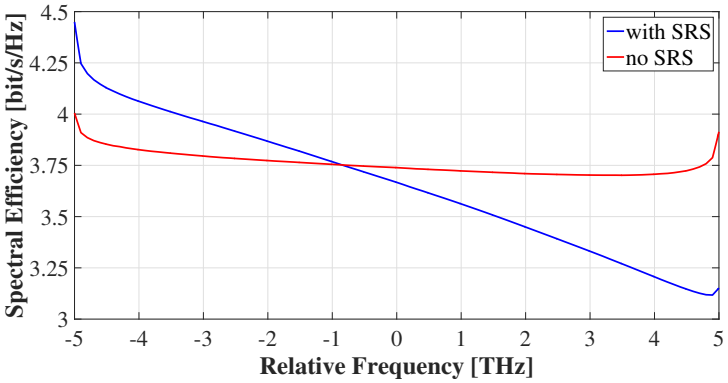


Fig. 5. Maximum achievable spectral efficiency of each channel in a 10 THz WDM signal.

the use of adaptive modulation formats and coding rates for each individual channel. This way the spectral efficiency can follow the channel dependent OSNR and system performance can be optimized. Tailoring coding rates of individual channels to their respective OSNR has been experimentally demonstrated in [24–27].

## 3. Closed-form approximation

In this section a closed-form expression is derived that gives the OSNR for each channel at the end of the link for signals that have total bandwidths of up to 15 THz. When the Raman gain is approximated by a linear function (obtained with a least square error method, first proposed in [5]) as shown in Fig. 1 and assuming that $\frac{\omega_p}{\omega_s} \approx 1$, an analytical solution of Eq. (1) is given by [28]

$$P_i(z) = P_i(0)\exp(-\alpha z)\frac{P_{\text{tot}}\exp\left[(i-1)C_R P_{\text{tot}}\hat{L}_{\text{eff}}(z)\right]}{\sum_{k=1}^{M} P_k \exp\left[(k-1)C_R P_k \hat{L}_{\text{eff}}(z)\right]}, \tag{8}$$

with

$$P_{\text{tot}} = \sum_{k=1}^{M} P_k, \tag{9}$$

$$\hat{L}_{\text{eff}}(z) = \frac{1-\exp(-\alpha z)}{\alpha}, \tag{10}$$

$$C_R = \frac{S_R B_{\text{ch}}}{2A_{\text{eff}}}, \tag{11}$$

where $P_k$ represents the input power of channel $k$ and $S_R$ the slope of the approximated Raman spectrum (taken from Fig. 1). Again we assume that the optimum launch power $P_0$ is uniform across the spectrum. The channel dependent ASE noise of the amplifier is then

$$P_{\text{ASE},i} = F h f B_{\text{ch}} \frac{P_0}{P_i(L)}. \tag{12}$$

For the Kerr effect contribution the dispersion slope and the small decrease in SNR at the edges of the WDM signal are neglected. A closed-form approximation for the NLIN coefficient is then

given as [18]

$$\eta_i = \frac{8}{27}\gamma^2 \alpha_{\mathrm{eff},i} L_{\mathrm{eff},i}^2 \frac{\mathrm{asinh}\left(\frac{0.5\pi^2|\beta_2|B_{\mathrm{tot}}^2}{\alpha_{\mathrm{eff},i}}\right)}{\pi|\beta_2|B_{\mathrm{ch}}^3}. \tag{13}$$

Different effective lengths $L_{\mathrm{eff},i}$ and attenuation coefficients $\alpha_{\mathrm{eff},i}$ for different channels are used again to account for SRS. One could enhance the accuracy and calculate the effective length in integral form by inserting Eq. (8) in Eq. (5). However, in order to obtain a closed-form expression, the power evolution is approximated by a linear function on a logarithmic scale. Figure 2 shows as an example the linear approximation of the highest frequency channel. An approximation of the effective attenuation coefficient can be then calculated as

$$\alpha_{\mathrm{eff},i} = \alpha - \frac{1}{L}\ln\left\{\frac{P_{\mathrm{tot}}\exp\left[(i-1)C_R P_{\mathrm{tot}}\hat{L}_{\mathrm{eff}}(L)\right]}{\sum_{k=1}^{M} P_k \exp\left[(k-1)C_R P_k \hat{L}_{\mathrm{eff}}(L)\right]}\right\}, \tag{14}$$

which is inserted in Eq. (5) to directly obtain $L_{\mathrm{eff},i}$. When all channels have the same input power ($P_{\mathrm{tot}} = MP_0$), the relation

$$\begin{aligned}&\frac{P_{\mathrm{tot}}\exp\left[(i-1)C_R P_{\mathrm{tot}}\hat{L}_{\mathrm{eff}}(z)\right]}{\sum_{k=1}^{M} P_k \exp\left[(k-1)C_R P_k \hat{L}_{\mathrm{eff}}(z)\right]} = \\ &\exp\left[\left(i-\frac{1}{2}M-\frac{1}{2}\right)C_R M P_0 \hat{L}_{\mathrm{eff}}(z)\right]\frac{M\sinh\left[\frac{1}{2}MC_R P_0 \hat{L}_{\mathrm{eff}}(z)\right]}{\sinh\left[\frac{1}{2}M^2 C_R P_0 \hat{L}_{\mathrm{eff}}(z)\right]},\end{aligned} \tag{15}$$

can be used and the OSNR can then be conveniently expressed in a closed-form expression as

$$OSNR_i = \frac{P_0}{\eta_i P_0^3 + FhfB_{\mathrm{ch}}\exp\left(\alpha_{\mathrm{eff},i}L\right)}\frac{1}{N_s}, \tag{16}$$

with the effective loss approximation

$$\begin{aligned}\alpha_{\mathrm{eff},i} = \alpha - \frac{1}{L}&\left[\left(i-\frac{1}{2}M-\frac{1}{2}\right)C_R M P_0 \hat{L}_{\mathrm{eff}}(L)\right] \\ &\ln\left\{\frac{M\sinh\left[\frac{1}{2}MC_R P_0 \hat{L}_{\mathrm{eff}}(L)\right]}{\sinh\left[\frac{1}{2}M^2 C_R P_0 \hat{L}_{\mathrm{eff}}(L)\right]}\right\},\end{aligned} \tag{17}$$

$$L_{\mathrm{eff},i} = \frac{1-\exp\left(\alpha_{\mathrm{eff},i}L\right)}{\alpha_{\mathrm{eff},i}}. \tag{18}$$

## 4. Achievable information rates

The model described in the previous section was applied to assess the impact of SRS on overall system performance. We choose the achievable information rate as a figure of merit, where the AIR per channel is calculated from the well-known formula [23]

$$C_i = 2B_{\mathrm{ch}}\log_2(1+OSNR_i), \tag{19}$$

where the factor 2 accounts for dual polarization transmission. The parameters from the previous section and a total transmission length of $N_s \cdot L$ of 3000 km are assumed.

Without the use of adaptive modulation formats and coding rates the total throughput solely depends on the channel with the worst OSNR. The total AIR is then the AIR of the worst channel multiplied by the number of channels. Figure 6 shows the total AIR when the power is optimal, when the power is taken from Eq. (4) (which means that the optimal launch power is taken without considering SRS) and finally the launch power is taken such that the OSNR drop due to SRS is 0.5 dB. The results were calculated by numerically solving Eq. (1), integrating the power evolutions to obtain the effective attenuation coefficients and numerically solving the GN-model. Additionally, the closed-form expression (see Eq. (16)) derived in the previous section is plotted. The closed-form expression shows good agreement with the numerical results. For bandwidths

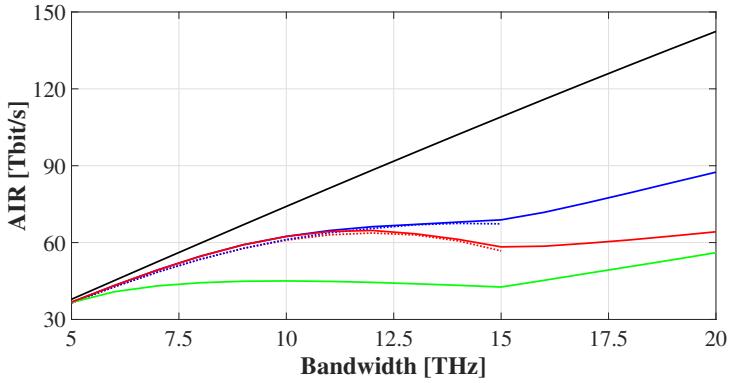


Fig. 6. Achievable information rate without adaptive modulation formats and coding rates at a transmission distance of 3000 km. Legend: —— No SRS. —— Numerical, optimal launch power. ····· Closed-form, optimal launch power. —— Numerical, launch power from Eq. (4). ····· Closed-form, launch power from Eq. (4). —— Numerical, SRS suppressed by low launch power.

of 10 to 15 THz, SRS significantly weakens the increase of AIR by bandwidth extension. Beyond 15 THz (peak of the Raman gain) it is again beneficial to increase the bandwidth even though the slope is slightly smaller than in the absence of SRS because the Raman gain coefficient does not vanish in this region. The achievable information rate due to SRS drops by approximately 40% for WDM signals with $B_{\text{tot}} > 15$ THz. Additionally, we confirm [6] that it is not optimal to suppress SRS by low launch powers (green curve).

The development of software-defined networking (SDN) could be a promising solution to the OSNR tilt introduced by SRS (Fig. 4). One could adaptively apply different modulation formats and coding rates for the different channels, maximizing the AIR of every channel. The total achievable information rate with adaptive modulation formats and coding rates is illustrated in Fig. 7. There is now only a small reduction in the AIR due to stimulated Raman scattering and bandwidth extension gives a substantial increase in performance over the entire investigated range. It is clearly not desirable to reduce SRS through the use of low powers (below the SRS thresholds) as this is far from the optimum. Operating in the presence of SRS and applying adaptive modulation and coding rates leads to a vast inrease in AIR. This is because SRS mainly introduces a tilt in the OSNR as shown in Fig. 4.

As for finding the optimum launch power, the simple Eq. (4) can be taken to compute the optimum launch power for bandwidths up to approximately 12.5 in the context of non-adaptive and up to 15 THz in the context of adaptive modulation formats and coding rates. The optimum launch power (blue curve) at a signal bandwidth of 15 THz and non-adaptive modulation formats

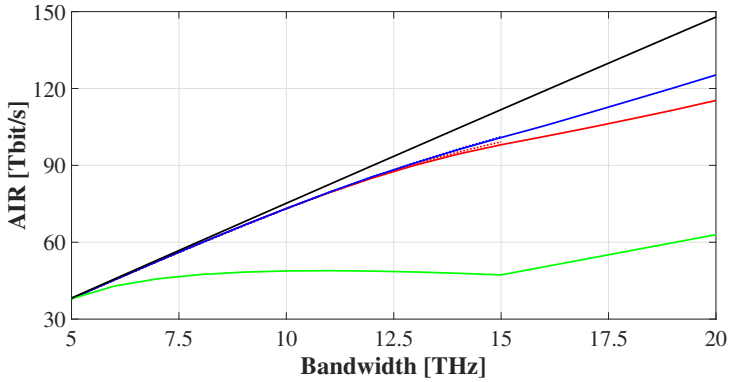


Fig. 7. Achievable information rate with adaptive modulation formats and coding rates at a transmission distance of 3000 km. Legend: —— no SRS. —— numerical, optimal launch power. ····· closed-form, optimal launch power. —— numerical, launch power from Eq. (4). ····· closed-form, launch power from Eq. (4). —— numerical, SRS suppressed by low launch power.

and coding rates is -10.1 dBm per channel and -8.1 dBm per channel in the case of adaptive modulation formats and coding rates. To keep the degradation in OSNR below 0.5 dB (green curve in Fig. 6 and 7 a launch power of -16.2 dBm per channel must be used. For comparison the standard GN model predicts an optimum launch power of -6.5 dBm per channel at a signal bandwidth of 15 THz. Generally, the optimum launch power in the presence of SRS is lower compared to the (theoretical) case of no SRS.

## 5. Conclusion

The impact of SRS on the achievable information rate was theoretically investigated in the context of ultra-wideband coherent Nyquist-spaced WDM communication systems, for the first time. If left unmitigated, SRS can significantly limit the potential throughput gains that can be achieved in future fully loaded C+L band systems and beyond. It was found that SRS introduces a reduction in achievable information rate of around 40% for bandwidths higher than 15 THz when a uniform modulation format and coding rate were used across the whole spectrum. The application of gain flattening filters, adaptive modulation formats and coding rates has been shown to limit the reduction in the achievable information rates to around 10% for bandwidths higher than 15 THz. In contrast to other proposed techniques, for example spectral inversion or the use of special fiber design, adaptive modulation formats and adaptive coding rates do not require major changes in the current network infrastructure. The solution may be particularly attractive in the context of software-defined networks, where adaptive modulation and coding may already be applied. A newly derived, closed-form, expression for the OSNR at the receiver (valid up to 15 THz), exhibiting excellent agreement with numerical calculations can be used for future system design and operation, to predict system performance and identify optimum launch powers.

In summary, stimulated Raman scattering introduces new challenges when extending the bandwidth of long-haul WDM systems, but will not impose insurmountable limitations. Effective mitigation techniques include the use of optimized wavelength-dependent gain, adaptive modulation formats and adaptive coding rates.

## 6. Funding information

Support from UK EPSRC programme grant UNLOC (EP/J017582/1) and a Doctoral Training Partnership (DTP) studentship to Daniel Semrau is gratefully acknowledged.